Colloid Polym Sci (2008) 286:417–426
DOI 10.1007/s00396-007-1788-4

ORIGINAL CONTRIBUTION

Decontamination of chemical warfare agents using perchloroethylene–Marlowet IHF–H_2O-based microemulsions: wetting and extraction properties on realistic surfaces

Stefan Wellert · Henrik Imhof · Michael Dolle · Hans-Jürgen Altmann · André Richardt · Thomas Hellweg

Received: 29 August 2007 / Revised: 16 October 2007 / Accepted: 16 October 2007 / Published online: 7 December 2007
© Springer-Verlag 2007

Abstract At the present time, considerable efforts are being made to develop new media for the decontamination of a variety of toxic compounds. In the present contribution, new microemulsions with promising properties are presented. Moreover, the decontamination of surfaces, with an emphasis on varnished metal surfaces of exterior and interior equipment, is investigated using these microemulsions. Studies of the phase behavior of the system water–perchloroethylene–IHF–2-propanol are reported and the microemulsion phases are recognized. The wetting behavior on contaminated surfaces and the extraction capabilities with respect to contaminants are essential for an efficient decontamination. Hence, suitable microemulsions are identified on the basis of these properties. The decontamination efficiency of these microemulsions is first estimated on the basis of the ability to wet typical chemical nonresistant varnished steel sheets, which are authentic model systems for real surfaces. Afterwards, promising microemulsions and, as reference, different solvents are tested with respect to their capability to solubilize sulfur-mustard agent, again using realistic surfaces contaminated with this chemical warfare agent. Several microemulsions are found, which have the desired properties.

Keywords Microemulsions · Decontamination · Chemical warfare agent · Solubility parameter · Contact angle · Wetting

S. Wellert · H. Imhof · T. Hellweg (✉)
Physikalische Chemie I, Universitätsstr. 30,
Universität Bayreuth, 95447 Bayreuth, Germany
e-mail: thomas.hellweg@uni-bayreuth.de

M. Dolle · H.-J. Altmann · A. Richardt
Armed Forces Scientific Institute for NBC Protection,
P.O. Box 1142, 29623 Munster, Germany

Introduction

Hazardous compounds like organophosphates can be found in agricultural drain waters or in industrial waste waters. Nerve agents are also organophosphates and can be released in case of terrorist attack (e.g. Sarin attack in Tokyo) or in case of warfare. Also, mustard agent (yperite) still represents a significant danger due to the large worldwide stock of ammunition. For these reasons, it is necessary to develop new versatile decontamination systems with higher efficiencies compared to the available media.

Decontamination is the physical removal of toxic materials and hazardous compounds from contaminated surfaces, solubilization of these contaminants in a solvent, and degradation to a noneffect dose. In recent years, a growing number of works have been published on this subject [see, e.g., 1–5], and one of the most promising carrier systems for active decontaminants is microemulsions [6–9]. However, most of the studies mentioned above focus on the investigation of kinetical or mechanistic aspects of the degradation [7–11] of the respective hazardous compound. Besides human skin, exterior and interior equipment, vehicles, technical devices, and buildings are also important objects for

decontamination. Chemical warfare (CW) agents like organophosphorous esters known as nerve agents and sulfur mustard are organic compounds of low polarity and low volatility. Additionally, most CW agents only exhibit a low solubility in the commonly used solvents, especially in water [12].

Hence, before the degradation of CW agents can take place in a decontamination liquid, a number of important steps already take place, which have not yet quantitatively or even semiquantitatively been investigated. Namely, these steps are wetting of the contaminated surface; extraction of the CW agent from surface coatings like, e.g., paints; and, finally, solubilization of the hazardous compound. In the present work, we present the first experimental data for these important steps, and we also discuss new microemulsion systems, which seem to be promising carrier systems for decontaminants (aqueous bleaching agents [3] or enzymes [13, 14]) due to their solubilization capacity and their wetting properties.

Background

An efficient decontamination system has to be compatible with the properties of the targeted CW agents. In Table 1, some important physical properties of frequently discussed CW agents are summarized. The ability of CW agents to penetrate into chemically nonresistant surface coatings and the complex interplay of physical and chemical properties related to the involved solid, liquid, and gaseous phases [15, 16] can lead to long persistence times. If a few weight percents of a polymer are added to a penetrating toxic agent, its persistence time is increased significantly and can reach several days [17]. Moreover, these CW agent–polymer mixtures usually exhibit high viscosities, also complicating the decontamination process.

In contrast to this, typical decontaminants (like, e.g., hypochlorite or H_2O_2) are soluble in water. This fact, the often hydrophobic nature of the contaminants, and the heterogeneity of the contaminated surfaces make the development of an efficient decontamination process a challenging task.

A decontamination medium has to be able to extract the toxic substances out of the contaminated surface and bring them into contact with the decontaminants, dissolved in an aqueous phase. If contaminants are of low water solubility, the degradation of the toxic substances takes place at the oil–water interface (see scheme in Fig. 1).

The only way to combine aqueous and organic phases in one medium is to form macroscopic emulsions or microemulsions. In a macroscopic emulsion, the dispersion of oil in water (o/w) or water in oil (w/o) is only kinetically stabilized, resulting in a limited lifetime due to coagulation; Ostwald ripening; and, finally, phase separation. Microemulsions are thermodynamically stable homogeneous mixtures of water and oil, stabilized by ionic or nonionic surfactant molecules. In some systems, a short- or medium-chain alcohol or also salt is added. From the importance of solubilization problems in a variety of applications, numerous publications on the subject of microemulsions arose in the past few decades. This is illustrated by the large number of review articles and the intense work concerning the fundamentals of the microstructure of microemulsions [20–26]. In addition, a vast number of publications treat practical aspects, i.e., the use of microemulsions in solvent extraction and liquid chromatography [27], cleaning applications, oil recovery, pharmaceutical [28] and cosmetical formulations [29], preparation of nanoparticles [30, 31], and their use as reaction media [32–34].

Since the 1980s, the use of a macroscopic emulsion has been established for decontamination applications by the German armed forces [35]. This macroscopic emulsion is composed of 15 wt.% perchloroethylene (PCE), 76.5 wt.% water, 7.5 wt.% calcium hypochlorite, and 1 wt.% emulsifier Marlowet IHF [35]. As already mentioned, such a macroemulsion is unstable.

Table 1 Physical properties of CW agents

CW agent	Lost	Tabun	Sarin	Soman	VX
Code name	HD	GA	GB	GD	VX
State of aggregation	Liquid	Liquid	Liquid	Liquid	Liquid
Density (g/cm^3)	1.27	1.073	1.102	1.0222	1.008
Freezing point (K)	287.45	223	217	231	$\geq$ 222
Saturation conc. (mg/m^3)	625 [a]	612	21,900	3,000 [a]	7×10^{-4} [a]
Volatility (mg/m^3)	610 [a]	328 [a]	16,091 [a]	3,900	10.5
Heat of vaporization (J/g)	393.56	330.09	334.93	303.12	327.63
Vapor pressure (Pa)	14.0	1.8	289.3	53.3	0.03
Water solubility (%)	0.06 [a]	9.8	any ratio	2.1 [a]	misc. $\leq$ 9.4 °C and at pH $\leq$ 6

Values are taken from the US Army [18] and Othmer and Kirk [19]. All values are given at 25°C except those denoted with superscript letter *a*. These are given for 20°C

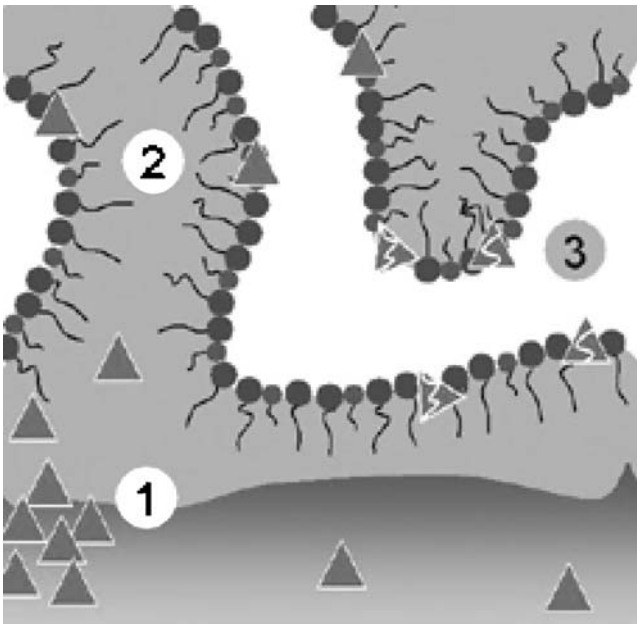

Fig. 1 Scheme of the decontamination process using a microemulsion as a carrier medium for the active component. The CW agent is extracted from the surface region (*1*) and dissolved in the oil component (*2*). At the oil–water interface, the decomposition of the CW agent takes place by reaction with the active agent dissolved in the water (*3*). The scheme reveals another important advantage of a microemulsion compared to a macroscopic one, which is the larger internal surface

Furthermore, the internal interface between water and oil is up to three orders of magnitude smaller in a macroemulsion compared to a chemically similar microemulsion system.

Therefore, since the 1990s, the use of microemulsions as a new approach for the decontamination of toxic chemical compounds has been discussed [17]. Some works extend the microemulsion concept to the decontamination of hazardous viruses and bacteria [36, 37]. Microemulsions of the o/w type using cyclohexane and hexadecane as the organic phase were reported to be efficient against mustard agent [38].

A continuous phase formed by propylene glycol and hydrogen peroxide extends the existence of the single-phase region to temperatures below 0 °C [39] for low-temperature decontamination. Besides the cheap and potent reactive component hypochlorite, chlorine-free agents like molybdate [8], magnetite nanoparticles [40], or magnesium monoperoxyphtalate and formamide [7] have also been reported as possible active reagents.

The aim of the present work is to develop a new versatile microemulsion carrier system for different active reagents that is able to wet all relevant surfaces equally well. Moreover, the components have to be cheap and available in large quantities. This is why the work presented here is based on the commercially available technical emulsifier Marlowet IHF.

Materials

Chemicals

The choice of an appropriate organic solvent as the "oil" component is essential for an efficient decontamination. The measurement of the solubilization behavior is complex and additionally complicated by the presence of CW agents. A rather simple and straightforward parameter that can be used to find an appropriate solvent for a CW agent is the Hildebrand solubility parameter δ [41, 42].

This parameter δ is the square root of the cohesive energy density c given by

$$c = \frac{\Delta H_{vap} - RT}{v_m} \tag{1}$$

and is calculated on the basis of the heat of vaporization ΔH_{vap}, the gas constant R, the temperature T at the boiling point, and the molar volume v_m [42]. This parameter reflects the degree of interaction between the molecules within a liquid. Low numbers, smaller than 20 $MPa^{1/2}$ reflect nonpolar interactions, while large numbers are observed for polar liquids, for example, 47 $MPa^{1/2}$ for water. In terms of this parameter, two liquids are miscible, if the difference of their Hildebrand parameters is very small, ideally close to zero.

Table 2 compares Hildebrand parameters for typical solvents and the most relevant CW agents. For example, it was observed that sulfur-mustard (HD) has a very low solubility in water of only 0.0043 mol/l [12], which corresponds to a large difference in the solubility

Table 2 Comparison of solubility parameters δ of typical solvents and some important CW agents [42–45]

	δ $(MPa)^{1/2}$
Solvent	
Toluene	18.2
Ethanol	26.0
Cyclohexane	16.8
Water	47.4
PCE	19.0
CW agent	
Tabun	18.8
Sarin	18.6
Soman	17.2
Lost (mustard)	21.9
VX	18.0

parameters due to the nature of the intermolecular forces acting in both liquids. For that reason, in this work, PCE is used as the "oil" component.

The commercially available emulsifier system Marlowet IHF (Sasol GmbH, Marl, Germany) was provided by the German armed forces. Marlowet IHF has a density of 1.06 g/cm^3, and its refractive index is 1.453. The used IHF is technical grade and contains 30 wt.% of a mixture of the nonionic oligo(ethylene oxide)alkyl ether surfactants, 53 wt.% of the ionic surfactant dodecylbenzenesulfonate Ca-salt, 15 wt.% 2-propanol, and 2 wt.% water. The fraction of the ionic surfactant in this mixture of ionic and nonionic surfactant is 0.64 and, therefore, assumed to dominate the phase behavior. The emulsifier has an averaged molar mass of 420 g/mol. PCE and 2-propanol were obtained from Sigma-Aldrich Chemie GmbH (Taufkirchen, Germany) with a purity > 99%. From the same company we purchased methylene diiodide, used as a standard for the contact angle measurements. Water was ultrapure deionized water (Milli-Q, Millipore, Billerica, MA, USA).

Substrates for the contact angle measurements and the decontamination tests

Contact angles were measured on silicon wafers, Teflon surfaces, and varnished metal sheets, representing an authentic model for "real" surfaces. These quadratic metal sheets have a side length of 10 cm. They are covered with a 50- to 150-μm layer of a paint commonly used for vehicles and equipment. Two different paints were studied here: a chemically resistant polyurethane paint (labeled with A, afterwards) and a chemically not-resistant alkyd varnish (denoted by B in the following). Additionally, weathered alkyd paint surfaces named C and D were also used for the experiments to produce even more realistic conditions. Similar metal sheets are also used for the determination of decontamination efficiencies.

Experimental methods

Phase behavior

All samples were prepared by weighing in the amounts of the components into sample tubes. They were mixed by sustained magnetic stirring and vortex mixing. Samples were equilibrated in thermostated baths and inspected visually in transmitted light to observe the phase behavior. The lamellar and the sponge-like bicontinuous phase were identified by using crossed polaroid filters.

In this work, the usual definitions [46] to specify the sample compositions are used. The fraction α of oil in the mixture of oil and water is

$$\alpha = \frac{m_{oil}}{m_{oil} + m_{water}} \tag{2}$$

and that of the emulsifier in the mixture of IHF and oil is

$$\beta = \frac{m_{IHF}}{m_{oil} + m_{IHF}} \tag{3}$$

The IHF masses are corrected for the 2-propanol content. The overall fraction of the alcohol is denoted as δ and given by

$$\delta = \frac{m_{alcohol}}{m_{oil} + m_{water} + m_{IHF} + m_{alcohol}}. \tag{4}$$

Similarly, the overall water content ω is defined. Overall fraction means that the 2-propanol content of the emulsifier is taken into account here.

Surface characterization

The varnished surfaces of the test metal sheets were inspected optically using a light microscope with an objective of 20-fold magnification (Carl Zeiss, Oberkochen, Germany). The surface roughness was measured with a Nanoscope III AFM (Digital Instruments, Tonawanda, NY, USA) in tapping mode with a OMCL-AC160TS standard silicon tip in air under ambient conditions. To determine the roughness parameter, defined as the root mean squared average of the height deviations, the image data were treated by using the NanoScope software version 5.12r5.

Contact angle measurements

An OCA 15 video-based optical contact angle meter (DataPhysics Instruments GmbH, Filderstadt, Germany) was used to measure the contact angles. Droplets of 10 μl volume, formed at the end of a needle, were brought into contact with the test surface. The contour of the homogeneous back-lightened droplets was recorded using a CCD-camera video system. Contact angles were calculated from the image data by a Young–Laplace fitting procedure. To avoid modifications of the surface layer, each test spot on the metal sheet was wetted only once. To cover a wide range of different environmental influences on the surface structure, ten independent sample sheets of type A, C, and D and 20 sheets of type B were used. Contact

angles were measured at three different positions on each sheet.

Decontamination efficiency

The decontamination efficiency was measured under special safety conditions in a high-security laboratory at the Armed Forces Scientific Institute, Munster, Germany, using sulfur-mustard (HD, S-Lost) as CW agent. HD was chosen due to its low volatility at room temperature and its ability to rapidly penetrate non-resistant surface coatings. The test surfaces used as substrates for these measurements were characterized before by contact angle measurements.

Equally spaced droplets of HD were placed on the test surfaces. The droplet volume was 1 μl, and the number of 80 droplets HD leads to a contamination density of 10 g m^{-2}. Evaporation of the CW agent can be neglected due to the low volatility and the storage of the sheets in a gas-tight box. A dwell time of 3 h was chosen, corresponding to realistic periods between contamination and decontamination.

After the dwell time elapsed, 10 ml microemulsion was sprayed on the contaminated steel sheets. The sheets were completely covered with the decontamination medium after application. After a residence/reaction time of 30 min, the medium was rinsed off with water and the decontaminated test sheets were dried with paper towels (Fripa Papierfabrik, Miltenberg, Germany).

The remaining contact and vapor risk is determined by the evaporation of the CW agent out of the decontaminated surface. To measure this evaporating amount, silica adsorber material, used in thin-layer chromatography (Fa. Merck, covered with silica gel 60), is placed and pressed on the surface with a load of 2,000 Nm^{-2}, simulating the intense contact of a human hand or arm with this surface . The desorbing CW agent is collected for 15 min, and subsequently, a mixture of 10 vol.% acetone and 90 vol.% heptane was used to extract the contaminants from the adsorber material. In addition, the same solvent mixture was also employed to extract residual remaining CW agent from the varnished test metal sheets.

The extraction time was 3 h for both the decontaminated steel sheets and the silica material. The gas chromatographic analysis (AutoSystem XL, Perkin-Elmer, Waltham, MA, USA, with flame ionization and flame photometric detectors) of the extracts from the adsorber material determines the contact and vapor risk R, while the analysis of the metal sheets gives the residual contamination r. All measurements were repeated with five different samples.

Results and discussion

The composition of the emulsifier Marlowet IHF is assumed as constant for all measurements reported here. Therefore, the IHF can be treated as a pseudo single component, and the resulting phase diagram for the pseudo quaternary system water–PCE–IHF–2-propanol can be represented by a tetrahedron, as schematically depicted in Fig. 2. Due to the constant content of 2-propanol in the emulsifier, the lower part of the tetrahedron was not accessible for the investigation of the phase behavior. This sector increases with increasing IHF content up to a value of $\delta_0 = 0.15$ in the binary system of 2-propanol and IHF. Sections at a constant PCE-water ratio α and a constant IHF–PCE ratio β were studied here and are marked with dash-dotted lines in Fig. 2. Additionally, the phase behavior of the four ternary systems, forming the surface of the phase tetrahedron, was investigated.

In Fig. 3, the measured phase diagrams of the four ternary mixtures forming the side faces of the tetrahedron are depicted. It is observed that PCE and water are immiscible within the experimental errors. The low-molecular-weight alcohol 2-propanol is completely miscible with water and PCE. Within the measured composition range, IHF is miscible with oil and water. When the fraction of IHF exceeded 25 wt.% in water and 40 wt.% in PCE, phases of high viscosity were found. This indicates the formation of mesoscopically organized structures at high surfactant content.

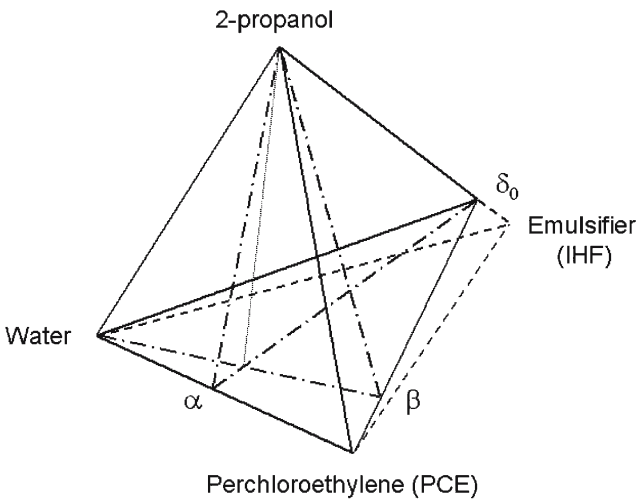

Fig. 2 Schematic-phase tetrahedron of the pseudoquaternary system water–PCE–IHF–2-propanol. As a result of the 2-propanol content δ_0 in the emulsifier IHF, not all points in the tetrahedron are reachable. The region that cannot be investigated is indicated by the *dotted lines*. The *dash-dotted lines* mark the sections through the tetrahedron at a constant water–oil ratio α and a constant IHF–PCE ratio β

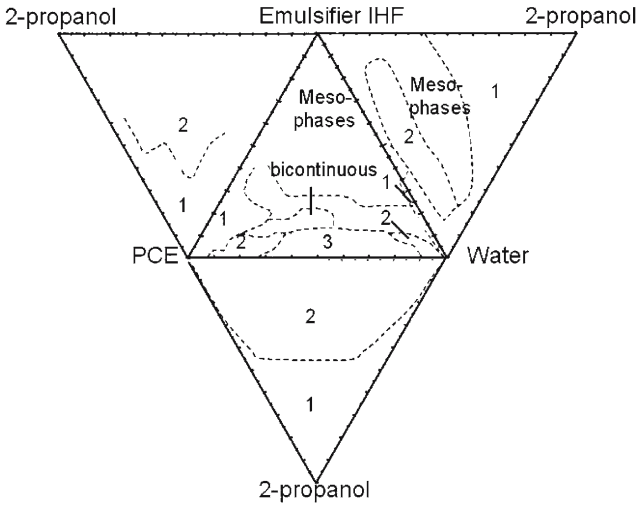

Fig. 3 Phase behavior in the four ternary-phase triangles representing the side faces of the water–PCE–IHF–2-propanol phase tetrahedron. In addition to the one-, two-, and three-phase regions, the bicontinuous phase and the range of the mesophases are depicted

In the ternary system water–PCE–IHF at low IHF contents, a large three-phase body is observed, accompanied by two-phase regions on both sides. In the oil-rich corner of the triangle, a single phase region of water-in-oil microemulsions exists. Increasing the fraction of IHF to 40 wt.% leads to partially birefringent highly viscous structures. These cannot be used for decontamination because, due to the high viscosity, they cannot easily be sprayed on contaminated surfaces, and they would have to be removed with a very large amount of water. Above the three-phase body, there exists a bicontinuous domain. This phase was identified by its flow birefringence between crossed polars. The observation of flow birefringence persists up to a water content of 50 wt.%. In the water-rich corner, a narrow, highly viscous single-phase channel is observed.

Figure 4 shows the rectangular representation of the phase diagram ("fish") at $\alpha = 0.62$. The contents of the emulsifier IHF and the 2-propanol were systematically varied at a temperature of 25 °C. Despite the rather complex composition and the technical grade of the emulsifier IHF, it is remarkable that typical phases and their sequences known from the Kahlweit-fish diagram first obtained for the pure nonionic surfactants of the C_iE_j type [46] can be reproduced when the alcohol content is used as tuning parameter for the curvature of the surfactant film.

This shows that the principles established for purified nonionic surfactants are very robust and also hold for multicomponent systems even containing impurities due to the use of technical soaps. The same result was found for quaternary systems containing purified and technical grade alkyl monoglucosides [47].

A large three-phase body ranging up to 9 wt.% of 2-propanol and 10 wt.% IHF is found. All expected one- and two-phase regions appear close to the three-phase body. The bicontinuous phase was observed in a range from about 11 to 20 wt.% IHF and at low contents of 2-propanol up to 4–5 wt.%. If the amount of the emulsifier is increased above 25 wt.%, the alcohol content exceeds 5 wt.% and the lamellar phase (L_α) occurs after passing the two-phase coexistence of the bicontinuous and the L_α phase. The single-phase region with a droplet microemulsion starts in a thin channel from the bicontinuous region and occurs at relatively high contents of 2-propanol.

In a second cut through the phase diagram, the amounts of 2-propanol and water were varied at $\beta = 0.29$ (see Fig. 5). In this pseudoternary phase diagram, a large one-phase region expands from the oil-rich corner. At nearly equal portions of water and oil, a bicontinuous channel was found. If more water was

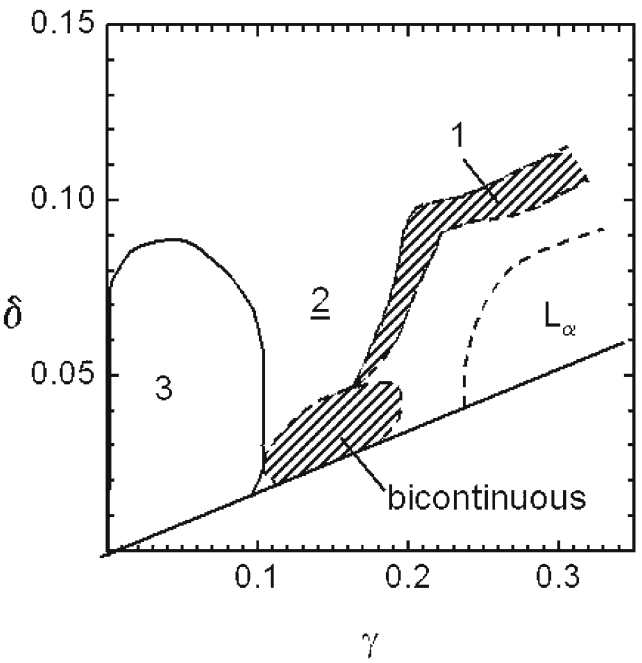

Fig. 4 Rectangular representation of a cut through the phase tetrahedron of the water–PCE–IHF–2-propanol system at $\alpha = 0.62$. As a result of the alcohol content in the emulsifier, the lower surfactant-rich corner is not accessible. *Hatched areas* are the oil-continuous (L_2 phase) and the bicontinuous 1-phase region. Additionally, two-phase, three-phase, and lamellar regions are indicated. The density of PCE is larger than the water density. Due to this, the commonly known sequence of phases found in, e.g., a test tube after demixing is inverted compared to the usual case. A water-excess phase is on top of the microemulsion phase, while an oil-excess phase appears on the bottom

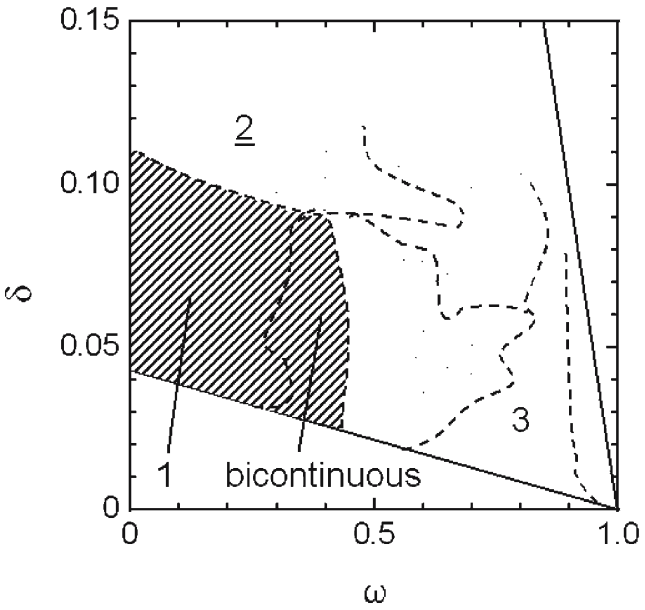

Fig. 5 Rectangular coordinate representation of a cut through the phase tetrahedron of the quaternary system water–PCE–IHF–2-propanol. While $\beta = 0.29$ is constant, δ and the overall water content ω were varied. The one-phase and the bicontinuous regions are indicated as *hatched areas*

added, two-phase and three-phase regions appeared. Only microemulsions from the one-phase region of this diagram were used in the experiments, as reported here.

Wetting properties

Although extraction of the contaminants out of the contaminated surface is the first important step in the decontamination process, previous published work focused on the degradation process [17, 48]. Real surfaces are heterogeneous and permanently exposed to various environmental influences. Such surfaces are, for example, the housing of technical equipment and vehicles, made of metal and varnished with chemically not-resistant, or sometimes also with resistant paints. In addition, it is desirable to wet hydrophobic and hydrophilic surfaces with the same decontamination medium.

Figure 6 shows optical microscope pictures and AFM images of surfaces of types A and B. The area investigated by optical microscopy (see pictures A1 and B1) is 0.5×0.5 cm. Both surfaces are not smooth but rather rough and qualitatively of similar heterogeneity on the length scales under consideration here. This length scale is comparable to the diameter of the area wetted by a droplet with a volume of a few microliters.

From the AFM images A2 and B2 in Fig. 6, the roughness parameter was determined at three different positions on the surfaces. For the surface of type A, a value of (26 ± 2) nm was found based on a scanned area of 80×80 μm. For the same scanned surface area, a somewhat smaller value of (16 ± 1) nm was obtained

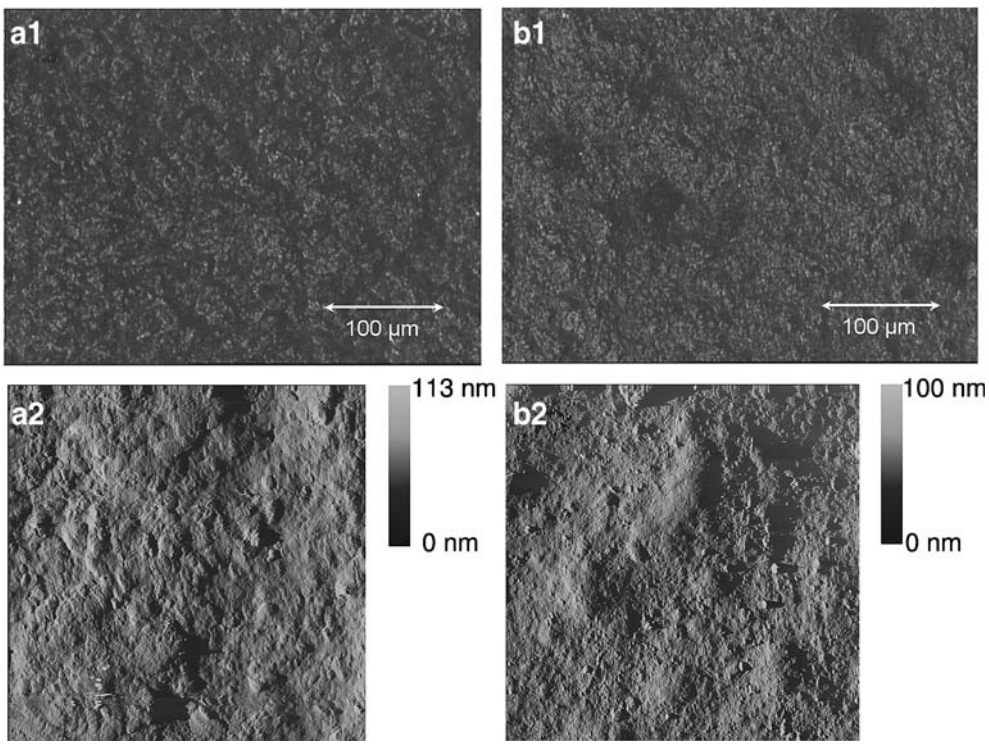

Fig. 6 Characterization of surfaces of type A and B with optical microscopy (**a1**, **b1**; scan size 0.5×0.5 cm) and measurement of AFM images (**a2**, **b2**; scan size 80×80 μm)

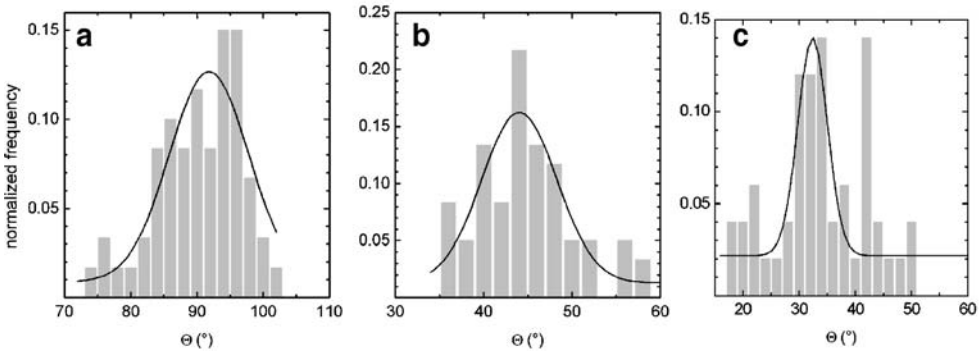

Fig. 7 Examples of contact angle distributions. **a** Water and **b** diiodomethane at polyurethane surfaces of type A; **c** microemulsion ME2 at alkyd paint surfaces of type D. Gaussian distribution was fitted to the data. The resulting mean values are **a** (91±10)°, **b** (44±9)°, and **c** (34±6)°

for a type B sample. However, both roughnesses are of the same order of magnitude.

As mentioned above, the use of real paints implies physical and chemical heterogeneities. Spreading coefficients, respectively, contact angles of polar and nonpolar liquids are a direct measure of the hydrophilicity or -phobicity of a surface [49, 50]. To cover a wide range of these random influences, contact angles θ of pure water and diiodomethane on varnished metal sheets of type A to D were measured, respectively. Figure 7 shows the distribution of contact angles determined from droplets at three different positions for 10 different sheets of surface types A and D. The resulting value for water is $\theta_A = (91 \pm 10)°$ as a result of a Gaussian fit (graph a) in Fig. 7). From diiodomethane, a value of $\theta_A = (44 \pm 9)°$ (graph b) was obtained. In graph c of Fig. 7, a typical contact angle distribution for the microemulsion ME2 is shown, and $\theta_D = (34 \pm 6)°$ was determined from the presented data. The contact angles for surface B are, for example, $\theta_B = (49 \pm 5)°$ for water and $\theta_B = (42 \pm 6)°$ for diiodomethane. Table 3 summarizes the results for the surface types A to D (the compositions of the used microemulsions are given in the caption of Table 3). Teflon and etched silicon wafers serve as a hydrophobic and hydrophilic reference. The values of water and diiodomethane for the surfaces A–D correspond to partially hydrophobic surfaces. For all measured surfaces, PCE contact angles were below the detection limit, which means that PCE is wetting all these different types of surface as a result of its nonpolar character and its low surface tension value, which is in contrast to the behavior of water. Microemulsions ME1 and ME2, used here, contain water and PCE in nearly equal portions, while in microemulsion ME3, less water was used. For all microemulsions, one might expect resulting contact angles between water and PCE. Indeed, this is approximately the result for the samples ME1 to ME3 (see Table 3).

The results are similar for all surfaces studied here and indicate that the prepared microemulsions sufficiently wet real heterogeneous varnished metal surfaces. From surface tension measurements using the Du Nuoy ring method values of $\gamma_L \approx 27$ mJ/m^2 are found for ME1 and ME2, which are just between water and PCE. This also explains the wetting behavior of the microemulsions with respect to the different tested surfaces. Obviously, the bicontinuous microemulsions wet all substrates used in this study.

Extraction and decontamination

Figure 8 shows the residual contents r of CW agent remaining in the paint on the surface after the treatment described in Section Decontamination efficiency for different pure solvents (listed in Table 2). The

Table 3 Contact angles on the different investigated surfaces A-D for polar and nonpolar liquids and microemulsions ME1 ($\alpha = 0.52$; $\gamma = 0.148$; $\delta = 0.026$), ME2 ($\alpha = 0.61$; $\gamma = 0.132$; $\delta = 0.055$) and ME3 ($\alpha = 0.93$; $\gamma = 0.234$; $\delta = 0.046$)

Liquid	γ_L^{LW} (mJ/m^2)	γ_L^{AB} (mJ/m^2)	θ_A (°)	θ_B (°)	θ_C (°)	θ_D (°)	θ_{teflon} (°)	θ_{wafer}
Water	21.8	51	91	49	59	64	120	≈ 0
Diiodomethane	50.8	0	44	42	35	36	81	46
PCE (C_2Cl_4)	32.0	0	≈ 0	≈ 0	≈ 0	≈ 0	≈ 0	≈ 0
ME1	–	–	38	38	45	47	37	38
ME2	–	–	32	26	38	34	36	26
ME3	–	–	28	22	20	22	35	19

The polar and nonpolar surface tension components γ_L^{AB} and γ_L^{LW} at 20° with $\gamma_L = \gamma_L^{AB} + \gamma_L^{LW}$ are given

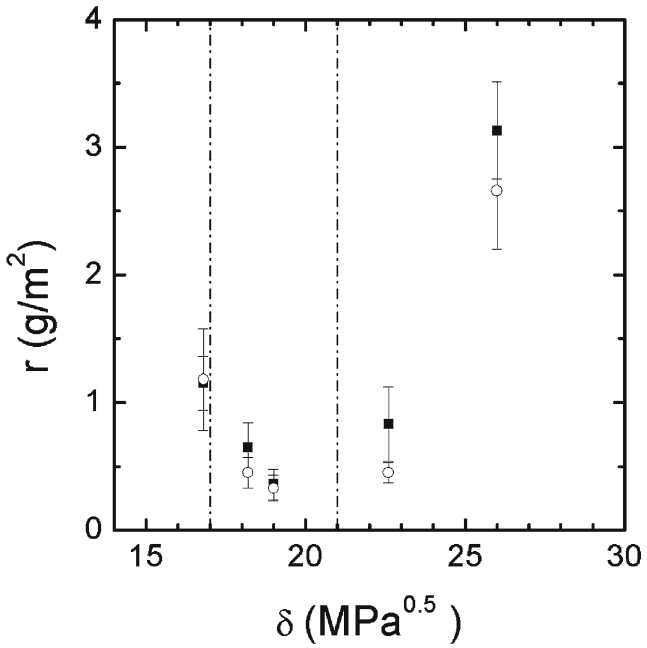

Fig. 8 Residual contents r for different pure solvents, represented by their Hildebrand solubility parameter. *Dashed lines* mark the upper and lower boundary of the solubility parameters of CW agents

values are given as a function of the respective Hildebrand solubility parameter. The dashed lines mark the interval of the solubility parameters of the most important CW agents as reported in the literature (see also Table 2). For example, PCE has a solubility parameter of 17.5 $MPa^{0.5}$ and shows, therefore, good extraction behavior leading to a residual content of (0.3 ± 0.1) g m^{-2}. In contrast to this, cyclohexane, a common solvent for microemulsion studies, has a residual content of (1.2 ± 0.4) g m^{-2} at a Hildebrand parameter of 16.8 $MPa^{0.5}$. For comparison, the threshold value for HD at a painted agent resistant surface is 0.60 g m^{-2}. Thus, extraction with the pure PCE already brings the contamination down to a harmless level and the CW agent is dissolved in the PCE.

The water domain in a microemulsion serves as the reservoir for additional active components like oxidizing agents, enzymes, or catalytic nanoparticles. Therefore, the decontamination efficiency of microemulsions with a high water content is of interest.

Table 4 summarizes the composition of different microemulsions with increasing oil fraction corresponding to a rising α. Microemulsions with low water content indicated by an α value close to unity are feasible, as well as microemulsions with a parameter $\alpha \approx 0.5$ and a bicontinuous structure. From the contamination density of 10 g m^{-2} used in our experiments, the size of the test sheets, and the microemulsion volume, used

Table 4 The decontamination efficiency for different microemulsions from the water–PCE–IHF–2-propanol system

α	γ	δ	R [g/(m^2 15 min)]	r (g/m^2)
0.487	0.138	0.096	0.16±0.09	0.085±0.015
0.520	0.148	0.026	0.13±0.03	0.055±0.011
0.610	0.132	0.055	0.15±0.05	0.070±0.014
0.928	0.235	0.094	0.49±0.17	0.082±0.026
0.930	0.234	0.046	0.48±0.26	0.071±0.030

The composition of the microemulsions is given in terms of α, γ, and δ

for the decontamination, an extraction capacity can be estimated. Taking the low solubility of HD in water into account, a concentration of ≈10 mg HD per 1 ml microemulsion is expected.

The comparably high contact-risk values, R, for the two last samples in Table 4 can be attributed to experimental uncertainties due to inhomogeneity of the series of the used test metal sheets. This also manifests in the large experimental errors for these samples. Taking this into account, one can conclude that the solubilization capacity of the solvent PCE is high enough to compensate for an increase of the water content at decreasing oil content in the system. Within these uncertainties, all prepared microemulsions are able to decontaminate HD spoiled surfaces, leading to an acceptable residual CW agent concentration and reasonable desorption values.

Conclusions

The phase behavior of the system PCE–water–IHF–2-propanol was investigated to transform the macroscopic emulsion currently used for this application into a more stable microemulsion. Although technical grade components were used, all phase regions and their typical sequence, known, for example, from ternary systems, using nonionic surfactants of the alkyl oligo ethyleneoxide type, can be reproduced. Hence, the present study reveals the robustness of the key concepts of microemulsion research, which were mainly established for purified model systems. All these concepts can still be applied to systems based on technical multicomponent soaps.

From studies of the phase behavior of this system, it was found that oil-continuous microemulsions are easily formed. The short-chain alcohol 2-propanol is an ingredient of the emulsifier IHF, and therefore, it seemed to be straightforward to use this alcohol to tune the curvature of the interfacial film in the studied

system. Also, this approach was successfully applied and all desired phases can be obtained as a function of 2-propanol concentration. However, due to its miscibility with water and PCE, 2-propanol acts as a cosolvent and tunes the curvature by changing the polarity of the solvent and not by changing the surfactant packing directly.

Microemulsions with nearly equal amounts of oil and water were found to wet standard and realistic model surfaces, which are partially hydrophobic. Additionally, the identified microemulsion phases were all found to be able to decontaminate surfaces loaded with mustard agent. In all cases, the residual content of the CW agent could be brought below the threshold, which indicates a danger for intoxication.

References

1. Lejeune KE, Dravis BC, Yang F, Hetro AD, Doctor BP, Russell AJ (1998) Ann N Y Acad Sci 864:153–170
2. Jaeger DA, III CLS, Zelenin AK, Li B, Kubicz-Loring E. (1999) Langmuir 15:7180–7185
3. Yang Y-C (1999) Acc Chem Res 32:109–115
4. Ghosh KK, Sinha D, Satnami ML, Dubey DK, Rodriguez-Dafonte P, Mundhara GL (2005) Langmuir 21:8664–8669
5. Wagner GW, Sorrick DC, Procell LR, Brickhouse MD (2007) Langmuir 23:1178–1186
6. Gonzaga F, Perez E, Rico-Lattes I, Lattes A (1999) Langmuir 15:8328–8331
7. Gonzaga F, Perez E, Rico-Lattes I, Lattes A (2001) New J Chem 25:151–155
8. Wagner GW, Procell LR, Yang Y-C, Bunton CA (2001) Langmuir 17:4809–4811
9. Tafesse F, Mndubu Y (2007) Water Air Soil Pollut 183: 107–113
10. Dubey DK, Gupta AK, Sharma M, Prabha S, Vaidyanathaswamy R (2002) Langmuir 18:10489–10492
11. Farquharson S, Gift A, Maksymiuk P, Inscore F (2005) Appl Spectrosc 59:654–660
12. Jackson KE (1934) Chem Rev 15:425–462
13. Lejeune KE, Swers JS, Hetro AD, Donahey GP, Russell AJ (1999) Biotechnol Bioeng 64:250–254
14. Richardt A, Blum M-M, Mitchell S (2006) Chem in Unserer Zeit 40:252–259
15. Love A, Vance A, Reynolds J, Davisson M (2004) Chemosphere 57:1257–1264
16. Groenewold G, Appelhans A, Gresham G, Olson J, Jeffrey M, Wright J (1999) Anal Chem 71:2318–2323
17. Yang Y-C, Baker J, Ward J (1992) Chem Rev 92:1729–1743
18. US Army (1990) Field maunal 3–9: potential military chemical/biological agents and compounds. Wiley, New York
19. Othmer DF, Kirk RE (1978) Encyclopedia of chemical technology. Wiley, New York
20. Kahlweit M et al (1987) J Colloid Interface Sci 118:436–453
21. Strey R (1994) Colloid Polym Sci 272:1005–1019
22. Langevin D (1992) Annu Rev Phys Chem 43:341–369
23. Hoffmann H (1994) Adv Mater 6:116–129
24. Gradzielski M, Langevin D, Sottmann T, Strey R (1996) J Chem Phys 104:3782–3787
25. Gelbart W, Ben-Shaul A (1996) J Phys Chem 100:13169–13189
26. Hellweg T (2002) Curr Opin Colloid Interface Sci 7:50–56
27. Watarai H (1998) J Chromatogr 780:93–102
28. Klier J, Tucker CJ, Kalantar TH, Green DP (2000) Adv Mater 12:1751–1757
29. Nakamura N, Tagawa T, Kihara K, Tobita I, Kunieda H (1997) Langmuir 13:2001–2006
30. Petit C, Lixon P, Pileni M (1993) J Phys Chem 97:12974–12983
31. Hellweg T, Eimer W (1998) Colloids Surf A 136:97–107
32. Schwuger M-J, Stickdorn K, Schomäcker R (1995) Chem Rev 95:849–864
33. Hao J (2000) Colloid Polym Sci 278:150–154
34. Lade O, Beizai K, Sottmann T, Strey R (2000) Langmuir 16:4122–4130
35. Altmann H-J (1989) German patent DE 3638625 C2. Deutsches Patentamt, Munich
36. Chepurnov AA, Bakulina LF, Dadaeva AA, Ustinova EN, Chepurnova TS, Baker JR (2003) Acta Trop 87:315–320
37. Hamouda T, Hayes MM, Cao Z, Tonda R, Johnson K, Wright DC, Brisker J, Baker JR (1999) J Infect Dis 180:1939–1949
38. Menger FM, Elrington AR (1990) J Am Chem Soc 112:8201–8203
39. Menger F, Rourk M (1999) Langmuir 15:309–313
40. Aubry JM, Bouttemy S (1997) J Am Chem Soc 119:5286–5294
41. Barton AFM (1975) Chem Rev 75:731–753
42. Barton AFM (1991) CRC handbook of solubility parameters and other cohesion parameters, 2nd ed. CRC Press: Boca Raton
43. Bellenger V, Morel E, Verdu J (1989) J Appl Polym Sci 37:2563–2576
44. Charlesworth JM, Riddell SZ, Mathews, RJ (1993) J Appl Polym Sci 47:653–665
45. Barlow JW, Paul D (1987)Polym Eng Sci 27:1482–1494
46. Kahlweit M, Strey R (1988) J Phys Chem 92:1557–1563
47. Kahlweit M, Busse G, Faulhaber B (1995) Langmuir 11:3382–3387
48. Wagner ZR, Roenigk TK, Goodson FE (2001) Macromolecules 34:5740–5743
49. Woodward JT, Gwin H, Schwartz DK (2000) Langmuir 16:2957–2961
50. van Oss CJ (1994) Interfacial forces in aqueous media narcel, 1st edn. Dekker, New York